Serial No. 06-1007B
Docket No. 50-339
Alternative Request CMP-023R1

ATTACHMENT 1

NON-PROPRIETARY

PWOL STRESS ANALYSIS CALCULATIONS FOR ALLOY 600 PRESSURIZER NOZZLE REPAIR

NORTH ANNA POWER STATION UNIT 2
VIRGINIA ELECTRIC AND POWER COMPANY (DOMINION)

AREVA

CALCULATION SUMMARY SHEET (CSS)

Document Identifier 32-9049431-000

Title North Anna Units 1 & 2 PZR Spray Nozzle Weld Overlay Crack Growth Evaluation

PREPARED BY:

NAME J. A. Brown

SIGNATURE [signature]

TITLE Advisory Engineer DATE 4/26/07

COST CENTER 41304 REF. PAGE(S) 35

REVIEWED BY:

METHOD: ☒ DETAILED CHECK ☐ INDEPENDENT CALCULATION

NAME H. P. Gunawardane

SIGNATURE [signature]

TITLE Engineer IV DATE 4/26/07

TM STATEMENT: REVIEWER INDEPENDENCE BD

NAME B. Djazmati

PURPOSE AND SUMMARY OF RESULTS:

Purpose: This document is a non-proprietary version of AREVA NP Document Number 32-9043015-000. The proprietary information removed form 32-9043015-000 is indicated by a pair of square brackets "[ ]". The geometry and operating conditions are Dominion Power proprietary. The purpose of the present analysis is to evaluate the fatigue crack growth of a partial through-wall 360° circumferential flaw into the Alloy 52M weld overlays at the North Anna Units 1 & 2 Pressurizer Spray Nozzle. This evaluation is performed at both the Alloy 82/182 butt weld joining the nozzle to safe end and the stainless steel weld joining the safe end to piping.

Results/Conclusion: After 33 years of operation, fatigue crack growth into the overlay material at both materials (Alloy 82/182 and stainless steel) is minimal and is summarized in the table below:

		DM WELD OVERLAY	SS WELD OVERLAY
Min WOL thickness,	t_{wol} =	[	
Additional WOL thickness required,	Δt_{wol} =		]
Initial flaw size,	a_i =	0.8750 in.	0.6850 in.
Final flaw size after 33 years,	a_f =	0.8927 in.	0.6881 in.
Flaw growth,	Δa =	0.0177 in.	0.0031 in.
Allowable crack depth to thickness ratio,	$(a/t)_{all}$ =	0.7500	0.7500
Final crack depth to thickness ratio,	$(a/t)_{final}$ =	0.7489	0.6437

The final configuration at the overlaid locations meets the Section XI, Appendix C acceptance criteria and the remaining ligament also satisfies basic applied membrane stress considerations.

THE FOLLOWING COMPUTER CODES HAVE BEEN USED IN THIS DOCUMENT:

CODE/VERSION/REV	CODE/VERSION/REV

THE DOCUMENT CONTAINS ASSUMPTIONS THAT MUST BE VERIFIED PRIOR TO USE ON SAFETY-RELATED WORK

☐ YES

☒ NO

RECORD OF REVISIONS

Revision	Affected Pages	Description of Revision	Date
000	All	Original release	04/07

TABLE OF CONTENTS

LIST OF TABLES

LIST OF FIGURES

1.0 Purpose

Due to the susceptibility of Alloy 600 and its associated weldments Alloy 82/182 to primary water stress corrosion cracking (PWSCC), Dominion plans to install a full structural weld overlay at the spray nozzle of the pressurizer at North Anna Units 1 and 2 (NA-1&2). A repair procedure has been developed where the dissimilar metal (DM) Alloy 82/182 weld and stainless steel (SS) safe end and weld, and a portion of both the nozzle and attached pipe are overlaid with PWSCC resistant Alloy 52M material, as shown in Figure 1. This repair design is more fully described by the overlay design drawing (Reference 1) and the technical requirements document (Reference 2). It is postulated that a 360° circumferential flaw would propagate by PWSCC through the thickness of the Alloy 82/182 weld, to the interface with the Alloy 52M overlay material. Qualification of the welding process (Reference 3) has demonstrated as-deposited weld metal chemistry sufficient to prevent PWSCC growth into the applied weld overlay and as such, no dilution layer is considered in this analysis. Although PWSCC would not continue to occur in the Alloy 52M overlay, it is further conservatively postulated that a small fatigue initiated flaw forms in the Alloy 52M overlay and combines with the PWSCC crack in the Alloy 82/182 weld to form a large partial through-wall full circumferential flaw that would propagate into the Alloy 52M overlay by fatigue crack growth under cyclic loading conditions.

A fracture mechanics analysis is performed to evaluate this worst case flaw in the repair configuration. This evaluation will consider sustained and normal/upset condition transient stresses (Reference 4) with the associated number of transient cycles to predict the final flaw size at the end of license extension at NA-1&2, which equates to a 33 year service life. This evaluation will demonstrate that the postulated circumferential flaw meets the ASME Code Section XI, Appendix C acceptance criteria (Reference 5, 14). An additional check will be made on the applied membrane stresses in the remaining ligament under normal operating conditions. This analysis is performed for both the Alloy 82/182 weld as well as the stainless steel weld joining the safe end to the piping.

Figure 1. Weld Overlay Configuration

2.0 Analytical Methodology

This analysis postulates a 360° circumferential flaw, which propagates by fatigue crack growth into the weld overlay, governed by a crack growth rate and stress intensity factor solution as detailed in Section 4.0. Applied stresses include both transient and sustained normal operating loads. The crack is grown on a yearly basis for 33 years.

As part of the overall effort in designing the weld overlay, a sizing calculation was prepared that determined the minimum thickness required to prevent net section collapse of the overlaid pipe (Reference 6). The sizing calculation design basis is a full circumferential through-wall flaw in the Alloy 82/182 butt weld or the stainless steel weld. The calculated minimum thickness does not take into account fatigue crack growth into the Alloy 52M weld overlay. This fracture mechanics calculation establishes the additional overlay thickness beyond the sizing calculation minimum requirement including the effect of a large initial flaw size and fatigue crack growth beyond this point while ensuring that the failure criteria detailed below are satisfied.

For highly ductile materials such as Alloy 52M, the acceptance criterion on flaw size is a 75% through-wall limit on depth (Reference 5, 15):

$$\frac{a}{t} \leq 0.75$$

Another acceptance criterion for ductile materials is demonstration of sufficient limit load margin. A limit load check is performed to ensure that net section collapse does not occur following crack growth as required by ASME B&PV Code, Section XI, Appendix C (Reference 5, 15).

Additionally, applied membrane stresses in the remaining ligament will be compared to the yield strength to ensure that failure will not occur due to axial pressure and piping loads under normal operating conditions.

Details of the methodology presented here are provided in Section 4.0 of this document.

3.0 Key Assumptions

There are no major assumptions for this calculation. Minor assumptions are noted where applicable.

The following engineering judgment is used in this analysis:

1. The fatigue crack growth rate for Alloy 600 material in a PWR environment (Reference 7, 8) modified by a multiplier of 2 based on Reference 9, can be used for Alloy 52M weld material in this analysis. Further discussion of this crack growth rate can be found in Section 4.4.

4.0 Calculations

4.1 Postulated Flaw Shape

A full circumferential partial through-wall internal flaw in a cylinder as shown in Figure 2 is postulated to exist at the time the overlay is applied. The flaw growth analysis contained within addresses the growth of the postulated flaw into the overlay material by cyclic loading.

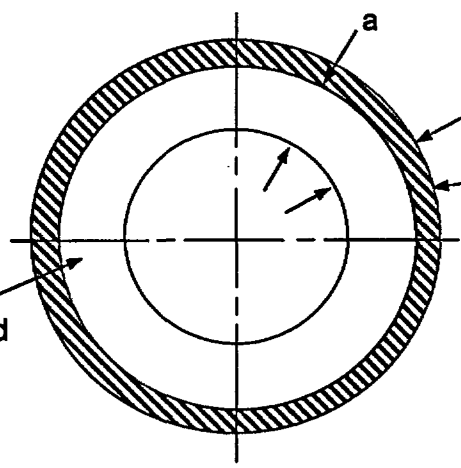

Figure 2. Internal Full Circumferential Partial Through-Wall Flaw

An axial flaw is considered to be bounded by the full circumferential partial through-wall internal flaw as shown in Figure 2 for several reasons. These include:

- Net section collapse of the axial flaw is not possible as the critical flaw size is very large.
- The axial flaw postulated is of 2:1 aspect ratio (length to depth) which generally results in a reduced stress intensity factor compared to a 360° circumferential flaw.
- The maximum length of an axial flaw is constrained by PWSCC resistant materials (the low alloy steel nozzle and stainless steel safe end).
- No external loads such as deadweight, thermal expansion or (tensile) shrinkage stresses are present in the hoop direction. Pressure stresses are accounted for in the transient stress results.
- Hoop residual stresses are less significant than axial residual stresses for crack growth.

4.2 Geometry

Basic dimensions at the safe end to nozzle dissimilar metal (DM) weld are

Outside diameter prior to overlay, [ ] in. (Reference 6)
Inside diameter, [ ] in. (Reference 6)

Basic dimensions at the safe end to piping SS weld are

Outside diameter prior to overlay, [ ] in. (Reference 6)
Inside diameter, [ ] in. (Reference 6)

4.3 Mechanical Properties

The yield strength for the Alloy 52M overlay material is tabulated below.

Table 1. Mechanical Properties of Alloy 52M

Condition	Temperature (°F)	Yield Strength, σ_y (ksi) ASME Code (Ref. 12)
Room Temperature	70	35.0
Normal Operating	[ ]	[ ]

The Design Stress Intensity (S_m) of the weld overlay material is 23.3 ksi at temperatures ranging from 100°F to 800°F.

4.4 Fatigue Crack Growth

Flaw growth due to cyclic loading is calculated using the fatigue crack growth model in the NRC flaw evaluation guidelines for Alloy 600 in a PWR environment (Reference 7, 8) which is based on work that was presented in NUREG/CR-6721 (Reference 9). Reference 9 shows that Alloy 52M materials do not exhibit the enhanced corrosion fatigue crack growth behavior of Alloy 82/182 materials in simulated 320°C PWR water. Instead, Alloy 52M behaves quite similarly to Alloy 600 in PWR water. However, to be conservative, a multiplier of 2 is applied to the Alloy 600 crack growth rate. Crack growth analysis is then conducted on a cycle-by-cycle basis to end of design life.

$$\frac{da}{dN} = 2 * C S_R S_{ENV} (\Delta K)^n \quad (1)$$

where ΔK is the stress intensity factor range in terms of $MPa\sqrt{m}$ and da/dN is the crack growth rate in terms of m/cycle

$$C = 4.835\text{x}10^{-14} + 1.622\text{x}10^{-16}T - 1.490\text{x}10^{-18}T^2 + 4.355\text{x}10^{-21}T^3 \quad (2)$$

$$S_R = [1 - 0.82R]^{-2.2}$$

$$S_{ENV} = 1 + A[CS_R\Delta K^n]^{m-1}T_R^{\,1-m}$$

$$A = 4.4\text{x}10^{-7}$$

$$m = 0.33$$

$$n = 4.1$$

$$T = \text{degrees C}$$

$$R = K_{min} / K_{max}$$

$$T_R = \text{rise time, set at 30 sec.}$$

4.5 Stress Intensity Factor Solution

The stress intensity factor used for an internal full circumferential partial through-wall flaw in a cylinder is the Buchalet and Bamford solution (Reference 13). This solution is based on an inside radius to thickness ratio of 10, which is conservative for the present configuration.

The stress intensity factor is:

$$K_I = \sqrt{\pi a}\ [A_0 F_1 + \frac{2a}{\pi} A_1 F_2 + \frac{a^2}{2} A_2 F_3 + \frac{4a^3}{3\pi} A_3 F_4], \quad (3)$$

A_0, A_1, A_2 and A_3 are coefficients of the third order polynomial stress distribution describing the axial stress (S(x)) variation through the cylinder wall given below:

$$S(x) = A_0 + A_1 x + A_2 x^2 + A_3 x^3 \quad (4)$$

where x is the distance measured from the inner surface of the cylinder wall.

F_1, F_2, F_3 and F_4 are geometry dependent magnification factors given by:

$$F_1 = 1.1259 + 0.2344(a/t) + 2.2018(a/t)^2 - 0.2083(a/t)^3$$
$$F_2 = 1.0732 + 0.2677(a/t) + 0.6661(a/t)^2 + 0.6354(a/t)^3$$
$$F_3 = 1.0528 + 0.1065(a/t) + 0.4429(a/t)^2 + 0.6042(a/t)^3$$
$$F_4 = 1.0387 - 0.0939(a/t) + 0.6018(a/t)^2 + 0.3750(a/t)^3$$

4.6 Applied Stresses

There are three categories of stress that need to be considered in this evaluation. Through-wall applied stresses in the axial direction are quantified. These stresses include:

- Transient through-wall stresses due to fluctuations in pressure and temperature
- Sustained stresses due to dead weight, piping thermal expansion, and axial shrinkage
- Welding residual stresses

The steady state stresses (i.e. sustained and residual) were combined with the stresses at each transient time point to develop the extreme (high and low) stress states for each transient. The combined through-wall stresses are fit to the third order polynomial described in the previous section.

4.6.1 Transient Stresses

The cyclic operating stresses that are needed to calculate fatigue crack growth were obtained from a linear-elastic three-dimensional finite element analysis (Reference 4). These fatigue stresses were developed for each of eight transients at a number of time points to capture the maximum and minimum stresses due to fluctuations in pressure and temperature. Per the technical requirements document (Reference 2), the number of RCS design transients established for the initial 40 year life is applicable to the 60 year licensed life of the plant (40 year design life plus 20 year life extension). Using the design transient cycle counts results in a conservative number of remaining plant cycles relative to the actual cycles of each transient that the plant has experienced during the period of operation up to the installation of the weld overlays.

Cyclic operating stresses were generated in Reference 4 for the eight transients listed below. The transient descriptions and cycle counts are given in Reference 4.

No.	Transient	Cycles over 60 years
1		
2		
3		
4		
5		
6		
7		
8		

Note [(1)]: Turbine Roll is a substep of HUCD. The HUCD also includes 4 independent spray events, one in heatup with 1000 occurrences and three in cooldown with 1200, 200, and 1000 occurrences respectively (Reference 15). The maximum number of cycles is conservatively set as the sum of the heatup/cooldown transient (200 cycles) plus the 2400 occurrences of cooldown spray activations, which equals 2600 events.

The above transients are grouped into six sets, as listed below. The bounding stresses from each set will be used to conservatively bound each group of cyclic loadings. An additional transient event due to seismic (OBE) loads is also included as a seventh transient. The high stress condition is taken to be the stresses due to each of these events applied at the steady state condition, such that the stresses are cycling between the maximum stresses and steady state are additional transients.

Group	Transient	Cycles over 60 years
1		
2		
3		
4		
5		
6		
7		

4.6.2 Sustained Stresses

The loads applied at the safe end (Reference 6, 15) are given below:

Table 2. Sustained Loads at the Safe End

Load Case	Forces (lbf)			Moments (in-lbf)			
	Axial	F_y	F_z	Torsion	M_y	M_z	SRSS
DW							
TH							
End Effects							
Total							

Note: The axial forces are aligned with the nozzle center line.

The loads applied at the safe end can be transferred to the nozzle by the moment arm of [ ] (Reference 6). The transferred results are listed in Table 3.

Table 3. Sustained Loads at the Nozzle

Load Case	Forces (lbf)			Moments (in-lbf)			
	Axial	F_y	F_z	Torsion	M_y	M_z	SRSS
DW							
TH							
End Effects							
Total							

Note: The axial forces are aligned with the nozzle center line.

4.6.3 Residual Stress in Welds

The residual stress profile through the thickness of the DM and SS welds and overlay is obtained from an analysis performed for the NA-1&2 safety and relief nozzles (Reference 10). Stresses were obtained over multiple paths through the thickness of the DM and SS welds and overlay. The paths over which these stresses are obtained are shown in Figure 3, and axial residual stresses are obtained over these paths. These stresses are combined with the transient stress results to obtain the combined stresses over the pathline. From this process, it was determined that the stresses at Path FR 4 were controlling for the DM weld. These results are used to perform the fatigue crack growth calculation.

Figure 3. Finite Element Model at DM and SS Welds with Pathlines Superposed

4.7 Flaw Growth Analysis

Flaw growth is calculated in one-year increments for each of the transient groups. The actual flaw growth analysis is presented in Table 6 for the DM weld and in Table 9 for the SS weld. For each table, the applied cycles are distributed uniformly over the service life by linking the incremental crack growth for each transient.

4.8 Limit Load Check

At the end of the flaw growth analysis, a limit load check is performed to ensure that net section collapse will not occur.

Per the ASME B&PV Code, Section XI, Appendix C (Reference 5, 14), only primary stresses (P_m and P_b) are considered. The primary stresses considered in this application result from internal pressure, dead weight and seismic loads (OBE or DBE). C-3320 of the same reference also specifies two sets of loading cases with different safety factors (*SF*) to be used: Normal/Upset (N/U) operating conditions (*SF* = 2.77), and Emergency/Faulted (E/F) conditions (*SF* = 1.39). The limiting load combinations for the N/U conditions are: internal pressure + DW + OBE. The limiting load combinations for the E/F conditions are: internal pressure + DW + DBE. Table 4 lists the maximum loads at the safe end (Reference 6). The loads applied at the safe end can be transferred to the nozzle by the moment arm of [ ] (Reference 6) and the results are listed in Table 5.

Table 4. Loading Conditions for Limit Load Check at Safe End

Load Case	Forces (lbf)(1)			Moments (in-lbf)			
	Axial	F_y	F_z	Torsion	M_y	M_z	SRSS
Internal Pressure(2)							
DW							
OBE (±)							
DBE (±)							
Total for N/U							
Total for E/F							

Note: (1) The axial forces are aligned with the nozzle center line
(2) Based on 2500 psia – conservative for all transients

Table 5. Loading Conditions for Limit Load Check at Nozzle

Load Case	Forces (lbf)(1)			Moments (in-lbf)			
	Axial	F_y	F_z	Torsion	M_y	M_z	SRSS
Internal Pressure(2)							
DW							
OBE (±)							
DBE (±)							
Total for N/U							
Total for E/F							

Note: (1) The axial forces are aligned with the nozzle center line
(2) Based on 2500 psia – conservative for all transients

For a circumferentially cracked pipe, the relation between the applied loads and the crack depth at incipient plastic collapse per References 5 & 14 is given by

$$P_b' = \frac{6S_m}{\pi}\left(2 - \frac{a}{t}\right)\sin\beta \qquad (7)$$

where t is the pipe thickness, β is the angle that defines the location of neutral axis (see Figure C-3320-1 of Appendix C, (Reference 5, 14) for details), and a is the crack depth. The assumed circumferential through-wall crack penetrates the compressive bending region such that $(\theta + \beta) > \pi$, where θ is the half crack angle. Therefore the angle β per References 5 & 14 is given by

$$\beta = \frac{\pi}{2 - \frac{a}{t}}\left(1 - \frac{a}{t} - \frac{P_m}{3S_m}\right) \qquad (8)$$

where P_m is the piping membrane stress in the axial direction in the uncracked section of the pipe. Per Reference 2 for a weld overlay using Alloy 52M, filler material shall be deposited using the ambient temperature temper bead machine GTAW process. The failure bending stress P_b' is therefore given by

$$P_b' = SF(P_m + P_b) - P_m \qquad (9)$$

with SF = 2.77 for Normal/Upset conditions and SF = 1.39 for Emergency/Faulted conditions. P_b is the piping bending stress in the intact section of the pipe. If the bending stress calculated using eqn. (7) exceeds that using eqn. (9) at the final crack depth, the component meets limit load requirements.

Results of the limit load check are shown in Table 7 and Table 10.

4.9 Applied Membrane Stress Check

This calculation verifies that the applied axial loads carried by the remaining ligament do not exceed yield stress at the final flaw size. Results are shown in Table 8 and Table 11.

5.0 Results and Conclusion

5.1 DM Weld Overlay

The stress intensity factors at the crack tip in the DM weld at the Alloy 52M weld overlay interface are calculated for each transient. Crack growth into the overlay is shown in Table 6 on the next page.

Table 6. Evaluation of Partial Through-Wall Circumferential Flaw in DM Weld Overlay

Table 6. Evaluation of Partial Through-Wall Circumferential Flaw in DM Weld Overlay (Cont'd)

Table 6. Evaluation of Partial Through-Wall Circumferential Flaw in DM Weld Overlay (Cont'd)

Table 6. Evaluation of Partial Through-Wall Circumferential Flaw in DM Weld Overlay (Cont'd)

Table 6. Evaluation of Partial Through-Wall Circumferential Flaw in DM Weld Overlay (Cont'd)

Table 6. Evaluation of Partial Through-Wall Circumferential Flaw in DM Weld Overlay (Cont'd)

Table 6. Evaluation of Partial Through-Wall Circumferential Flaw in DM Weld Overlay (Cont'd)

Table 6. Evaluation of Partial Through-Wall Circumferential Flaw in DM Weld Overlay (Cont'd)

Table 6. Evaluation of Partial Through-Wall Circumferential Flaw in DM Weld Overlay (Cont'd)

Flaw Sizes

Initial flaw size,	a_i = 0.8750 in.
Final flaw size after 33 years,	a_f = 0.8927 in.
Flaw growth,	Δa = 0.0177 in.
Final crack depth to thickness ratio,	a/t = 0.7489

Results of Limit Load Check

Table 7. Limit Load Results at DM Weld Overlay

Parameters	Description	N/U	E/F
d_o, inch	WOL outside diameter		
d_i, inch	Inside diameter		
a_f, inch	Final crack depth		
F, lbf	Axial force		
M, in-lbf	SRSS moment		
t_{wol}, inch	Weld overlay thickness		
t, inch	Overall thickness including weld overlay		
A, inch^2	Sectional area		
Z, inch^3	Section modulus		
P_m, psi	Membrane stress		
P_b, psi	Bending stress		
SF	Safety factor, Reference 4	2.77	1.39
P_b', psi	Failure bending stress by eqn. (7)		
P_b', psi	Failure bending stress by eqn. (9)		
a/t	**Final crack depth to thickness ratio**	**0.7489**	**0.7489**

Results of Applied Membrane Stress Check

Table 8. Applied Membrane Stress Check at DM Weld Overlay

Parameters	Description	Value
d_o, inch	WOL outside diameter	
t_{rem}, inch	Remaining ligament thickness	
F, lbf	Axial force (DW + TH + Pressure)	
A_{rem}, inch^2	Sectional area of ligament	
P_{ml}, psi	Membrane stress in ligament	
σ_y, psi	650°F yield stress in ligament	
	Margin	**2.08**

5.2 SS Weld Overlay

The stress intensity factors at the crack tip in the stainless steel weld to Alloy 52M weld overlay interface were calculated for each transient. The initial flaw is assumed conservatively to have propagated along the SS weld HAZ rather than radially outward from the weld root. This is consistent with the overlay thickness sizing calculations (Reference 6). With this crack path the initial flaw depth is [ ] in. For all transients, other than the [ ] transients, the highest and lowest stress intensity factors were negative, which indicates that no fatigue crack growth is possible. For the remaining transients [ ], crack growth into the overlay is shown in Table 9 on the next page.

Table 9. Evaluation of Partial Through-Wall Circumferential Flaw in SS Weld Overlay

Table 9. Evaluation of Partial Through-Wall Circumferential Flaw in SS Weld Overlay (Cont'd)

Table 9. Evaluation of Partial Through-Wall Circumferential Flaw in SS Weld Overlay (Cont'd)

Table 9. Evaluation of Partial Through-Wall Circumferential Flaw in SS Weld Overlay (Cont'd)

Flaw Sizes

Initial flaw size,	a_i = 0.6850 in.
Final flaw size after 33 years,	a_f = 0.6881 in.
Flaw growth,	Δa = 0.0031 in.
Final crack depth to thickness ratio,	a/t = 0.6437

Results of Limit Load Check

Table 10. Limit Load Results at SS Weld Overlay

Parameters	Description	N/U	E/F
d_o, inch	WOL outside diameter		
d_i, inch	Inside diameter		
a_f, inch	Final crack depth		
F, lbf	Axial force		
M, in-lbf	SRSS moment		
t_{wol}, inch	Weld overlay thickness		
t, inch	Overall thickness including weld overlay		
A, inch^2	Sectional area		
Z, inch^3	Section modulus		
P_m, psi	Membrane stress		
P_b, psi	Bending stress		
SF	Safety factor, Reference 4	2.77	1.39
P_b', psi	Failure bending stress by eqn. (7)		
P_b', psi	Failure bending stress by eqn. (9)		
a/t	**Final crack depth to thickness ratio**	**0.6437**	**0.6437**

Results of Applied Membrane Stress Check

Table 11. Applied Membrane Stress Check at SS Weld Overlay

Parameters	Description	Value
d_o, inch	WOL outside diameter	
t_{rem}, inch	Remaining ligament thickness	
F, lbf	Axial force (DW + TH + Pressure)	
A_{rem}, inch^2	Sectional area of ligament	
P_{ml}, psi	Membrane stress in ligament	
σ_y, psi	650°F yield stress in ligament	
	Margin	**3.20**

5.3 Conclusion

After 33 years of operation, fatigue crack growth into the overlay material at both locations is minimal and is summarized in the table below:

		DM WELD OVERLAY	SS WELD OVERLAY
Min WOL thickness,	t_{wol} =		
Additional WOL thickness required,	Δt_{wol} =		
Initial flaw size,	a_i =	0.8750 in.	0.6850 in.
Final flaw size after 33 years,	a_f =	0.8927 in.	0.6881 in.
Flaw growth,	Δa =	0.0177 in.	0.0031 in.
Allowable crack depth to thickness ratio,	$(a/t)_{all}$ =	0.7500	0.7500
Final crack depth to thickness ratio,	$(a/t)_{final}$ =	0.7489	0.6437

The final configuration at the overlaid locations meets the Section XI, Appendix C (Reference 5, 14) acceptance criteria and the remaining ligament also satisfies basic applied membrane stress considerations.

6.0 References

1. AREVA Drawing 02-8017175D-001, "North Anna Pressurizer Spray Nozzle Overlay Design."

2. AREVA Document 51-9031151-002, "North Anna Units 1 and 2 Pressurizer Nozzle Weld Overlays – Technical Requirements."

3. AREVA Document 51-9009149-004, "Alloy 52 Overlay Chemistry Results."

4. AREVA Document 32-9035736-001, "North Anna Units 1 and 2 Pressurizer – Spray Nozzle Weld Overlay Analysis."

5. ASME Boiler and Pressure Vessel Code, 1989 Edition, Section XI, Division 1.

6. AREVA Document 32-9034391-003, "North Anna Units 1 & 2 Pressurizer Weld Overlay Sizing Calculation – Spray Nozzle."

7. NRC Letter from Richard Barrett, Director Division of Engineering, Office of NRR to Alex Marion of Nuclear Energy Institute, "Flaw Evaluation Guidelines," April 11, 2003, Accession Number ML030980322.

8. Enclosure 2 to Reference 7, "Appendix A: Evaluation of Flaws in PWR Reactor Vessel Upper Head Penetration Nozzles," Accession Number ML030980333.

9. NUREG/CR-6721, "Effects of Alloy Chemistry, Cold Work, and Water Chemistry on Corrosion Fatigue and Stress Corrosion Cracking of Nickel Alloys and Welds," U.S. Nuclear Regulatory Commission (Argonne National Laboratory), April 2001.

10. AREVA Document 32-9044883-000, "North Anna Units 1 and 2, Pressurizer Spray Nozzle Weld Residual Stress Analysis."

11. AREVA Drawing 02-8016864C-005, "North Anna Unit Pressurizer Spray Nozzle Design."

12. ASME Boiler and Pressure Vessel Code, 2001 Edition including Addenda through 2003, Section II, Part D.

13. C.B. Buchalet and W.H. Bamford, "Stress Intensity Factor Solutions for Continuous Surface Flaws in Reactor Pressure Vessels," Mechanics of Crack Growth, ASTM STP 590, American Society for Testing and Materials, 1976, pp. 385-402.

14. ASME Boiler and Pressure Vessel Code, 1995 Edition including Addenda through 1996, Section XI, Division 1.

15. AREVA Document 51-9036969-004, "Pressurizer Bounding Transients for North Anna Units 1 & 2."

7.0 Computer Output

Not applicable.